Biosensors and Bioelectronics 141 (2019) 111432

Contents lists available at ScienceDirect

Biosensors and Bioelectronics

journal homepage: www.elsevier.com/locate/bios

A SERS-based lateral flow assay biosensor for quantitative and ultrasensitive detection of interleukin-6 in unprocessed whole blood

Ying Wang[a], Jingyi Sun[b], Yajun Hou[a], Cheng Zhang[a], Dawei Li[a], Hanxia Li[a], Mingfeng Yang[a], Cundong Fan[a,**], Baoliang Sun[a,*]

[a] Key Lab of Cerebral Microcirculation in Universities of Shandong, Shandong First Medical University & Shandong Academy of Medical Sciences, Taian, Shandong, 271000, China

[b] Wonju Severance Christian Hospital, Yonsei University Wonju College of Medicine, Wonju, Gangwon, 220-701, Republic of Korea

ARTICLE INFO

Keywords:
Core-shell SERS nanotags
Gold nanoparticles
DTNB
Cytokines
Biomarker
Point-of-care-testing

ABSTRACT

Detection of a very low amount of cytokines such as interleukin-6 (IL-6) in clinical fluids such as blood is important in biomedical research and clinical applications. A surface-enhanced Raman scattering (SERS)-based lateral flow assay (LFA) is developed for the quantitative analysis of IL-6. The Raman reporter 5,5′-dithiobis-2-nitrobenzoic acid (DTNB) on gold nano shell with a silica core was employed as the SERS tags. They are shown to perform much better than colloidal gold in LF strips. The IL-6 protein can be detected by this method with very low detection limits by monitoring the intensity of the characteristic Raman peak of the IL-6-conjugated SERS tags at 1332 cm^{-1}. Under optimized conditions, the assay works in the 1 pg/mL to 1 μg/mL IL-6 concentration range, and the detection limit is as low as 1 pg/mL in PBS, 5 pg/mL in unprocessed whole blood. This is lower by a factor of 3 compared to colorimetric or fluorimetric methods. The performance of SERS LFA was demonstrated by detection of IL-6 in unprocessed whole blood with comparable performance of the conventional enzyme-linked immunosorbent assay (ELISA).

1. Introduction

The immune system is an interactive network of lymphoid organs, cells, humoral factors, and cytokines. Each element performs a specific task in host defence aimed at recognizing and/or reacting against 'foreign material'. Disorders of the immune system can result in autoimmune diseases, allergic, the severe infections and tumours of immunodeficiency (Parkin and Cohen, 2001). Approximately 3% of the human population is affected by a recognized autoimmune disorder (Gregersen and Behrens, 2006). Therefore, development of new methods of quantitative analysis of immune markers will lead to a better understanding of immune system disorders and should open new avenues for therapeutic regimens.

Cytokines play a key role in both immunosuppression and immunoenhancement. Interleukin-6 (IL-6), is a 21 kDa glycoprotein referred to as a pro- and an anti-inflammatory cytokine because it has multifunction which act in both pathways (Russell et al., 2019). Up to now several analytical procedures (bioassay, immunoassay, molecular biology technique, flow cytometry) have been applied for evaluating cytokine levels in body fluids, tissues, and cells; of these the commercial Enzyme-linked immunosorbent assays (ELISA) is most often used (Corsini and House, 2018). Especially in clinical protein determinations, but the sensitivity of ELISA is low and it suffers from some interference (Shi et al., 2014). Additionally, the problems of reducing the sample volume and increasing sensitivity and stability of the sensing system still remain unsolved (Zhang et al., 2018). Interleukins such as IL-6 in body fluids usually circulate in tiny amounts (nano- and picomolar) and their concentrations can increase up to 1000-fold when immune system activation is required (Kamińska et al., 2017). Therefore, it is essential to develop and optimize new technologies for quantitative detection of IL-6 for research and clinical applications.

A paper-based lateral flow assay (LFA) have been considered the most widely used point-of-care-testing (POCT) diagnostics due to low costs, rapid analysis, and userfriendly format (Wang et al., 2017; Lopez et al., 2016). The major drawback of this assay is the limited detection sensitivity and qualitative ability based on colorimetric analysis, which made these LFA biosensors less attractive (Rong et al., 2018; Van Hooij et al., 2016). To resolve these problems associated with LFA, we developed a novel surface-enhanced Raman scattering (SERS)-based LFA for the quantitative analysis of a specific biomarker in the low

* Corresponding author.
** Corresponding author.
E-mail addresses: cdfan@tsmc.edu.cn (C. Fan), blsun@tsmc.edu.cn (B. Sun).

https://doi.org/10.1016/j.bios.2019.111432
Received 21 March 2019; Received in revised form 4 June 2019; Accepted 10 June 2019
Available online 19 June 2019
0956-5663/

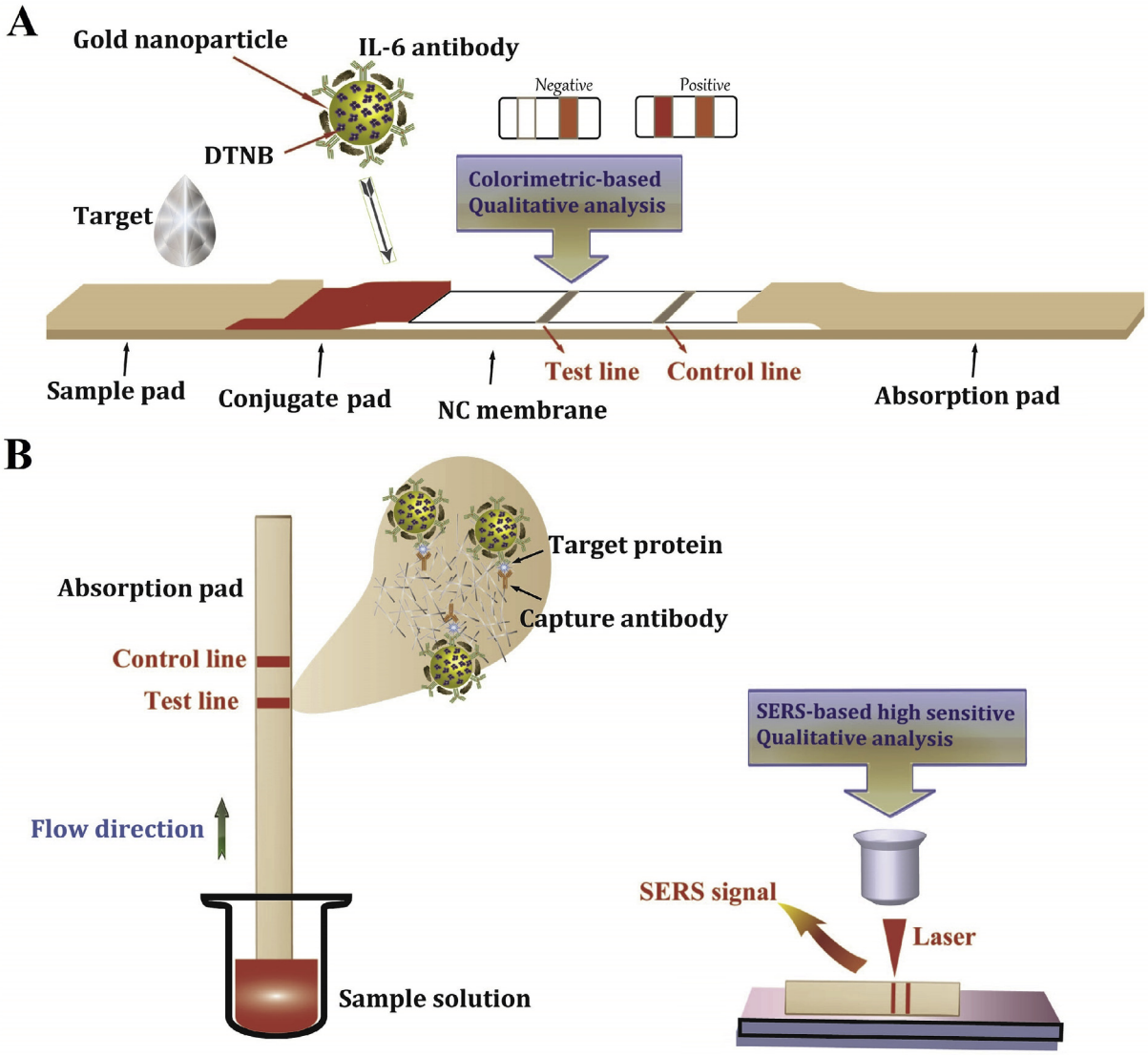

Scheme 1. (A) Schematic illustration of the configuration and (B) the measurement principle of the SERS-based lateral flow assay for quantification of IL-6.

concentration range (Fu et al., 2016).

SERS is a powerful platform for selective detection of biomolecules with a single molecule-level sensitivity (Xie et al., 2018). Compared with traditional immunoassays, SERS has some especial advantages (Wang et al., 2013). Firstly SERS has better selectivity ability to target molecules in real complex sample system due to its fingerprint characteristic (Li et al., 2019; Wang et al., 2018a,b). Second SERS can highly amplified and quantifiable the Raman signals of with good stability, convenience and reproducibility (Chen et al., 2018; Mao et al., 2009). As a result, SERS has been widely used in the detection of proteins for immunoassays (Khlebtsov et al., 2019; Guerrini et al., 2015).

Herein, we propose a novel SERS-based LFA for the quantitative analysis of IL-6 in the unprocessed whole blood. In this system, anti-IL-6 antibody and Raman molecules (5,5′-Dithiobis-2-nitrobenzoic acid (DTNB))-functionalized Au NPs were used as SERS tags. DTNB was used as Raman reporter molecule due to its strong Raman enhancement effect (Zhao et al., 2019; Pang et al., 2019). The SERS tags displayed stronger SERS signals with the enhancement factor of 1.5×10^7, and processed excellent stability in the unprocessed whole blood solutions. These SERS tags were used as an alternative to the colloidal gold that are utilized in conventional LFA (Hwang et al., 2016; Zhang et al., a). Quantitative analysis of IL-6 can be performed by recording the Raman intensity change on the test line (Tran et al., 2019). Compared to the commercial ELISA, the SERS-based LFA shows much higher sensitivity in the unprocessed whole blood. These results can evaluate the feasibility of our approach in clinical application, which show a great potential of SERS-LFA in the POCT setting.

2. Materials and methods

2.1. Materials

N-hydroxysuccinimide (NHS), γ-amino-propyl-triethoxysilane (APTES), 1-[3-(dimethylamino)propyl]-3-carbodiimide hydrochloride (EDC), 5,5′-Dithiobis-2-nitrobenzoic acid (DTNB), Tetrakis(hydroxymethyl)phosphonium chloride (THPC) and goat anti-mouse IgG antibody were purchased from Sigma-Aldrich Chemicals. Dimercaptosuccinic acid (DMSA), ethanol, K_2CO_3 and Phosphate buffer saline (PBS) were purchased from Aladdin Bio-Chem technology LTD (Shanghai, China). Chloroauric acid terahydrate ($HAuCl_4$), hydrogen peroxide (H_2O_2) (30%), Bovine serum albumin (BSA) were purchased from Shanghai Chemical Reagent LTD (Shanghai, China). The silica colloidal particles (SiO2) were obtained from Nissan Chemical Corporation, Japan. IL-6 standard grade antigen, anti-IL-6 mouse

monoclonal antibody were purchased from Linc-Bio Science LTD (Shanghai, China). Human blood samples were kindly provided by the Affiliated Hospital of Taishan Medical University. All other used chemical reagents were of analytical grade or higher and used without further purification. Milli-Q-grade water (18.2 MΩ cm) was used for all experiments.

2.2. Synthesis of AuNPs

Briefly, silica (SiO_2, 0.013 g/mL) was firstly dispersed in 40 mL of ethanol and amino-functionalized by APTES (1% v/v in ethanol) at 80 °C. Tiny gold nanoparticles (~2 nm) were synthesized by $HAuCl_4$ using THPC reducing agent at room temperature (Tharion et al., 2015). Functionalized SiO_2 NPs was added to gold nanoparticles under stirring to form SiO_2/Au NPs composites. The growing solution was prepared by mixing 750 mL deionized water, 200 mg of K_2CO_3, and 12 mL of 1% $HAuCl_4$ and stirring for 30 min SiO_2/Au NPs composites and H_2O_2 were added in turn to growing solution while stirring. The AuNPs were concentrated by centrifugation at 3000 rpm for 20 min and redispersed in 10 mL of water for further use.

2.3. Synthesis of IL-6 labeling antibody modified SERS active Au NPs-tags

Nanoparticles were washed by distilled water twice. 100 μL as-prepared Au NPs were dispersed in 400 μL distilled water. Then co-incubate with 60 μL DTNB aqueous solution (10^{-3} mol/L) for 30 min. The DTNB adsorbed Au NPs were re-dispersed in 500 μL PBS (containing 2 mM DMSA), and activated by freshly prepared mixture solution containing 30 mM NHS and 150 mM EDC. Then, 20 μL IL-6 labeling antibody (10 μg/mL) was added and incubated for 1 h. Subsequently, the functionalized SERS tags (Au@DTNB@IL-6-antibody NPs) were purified by centrifuged at 6000 rpm for 10 min to remove excess unconjugated chemicals and antibodies. At last, 1% BSA was added to block the unbound surfaces of Au NPs as shown in Scheme 1A.

2.4. Preparation of the IL-6 probe-immobilized LFA

A schematic diagram of the SERS based LFA sensor prepared in this work is shown in Scheme 1A. The SERS-based LFA sensor consisted of four sections: sample pad, conjugate pad, NC membrane (test and control lines), and absorption pad. The sample pad was blocked with 20 mM Tris-HCl containing 0.25% TRITON X-100 and 150 mM NaCl, followed by overnight drying at 37 °C to ensure optimal conditions for the analytes throughout the flux. The conjugated pad was prepared by addition of 6 μL of SERS tags and dried at room temperature. The test (T) line and control (C) line were drawn with anti-IL-6 antibody and goat anti-mouse IgG antibody on NC membrane, respectively. Leaving a 0.5 cm space between the two lines, and dried at room temperature for 1 h. Then sample pad, conjugate pad, NC membrane and absorption pad were assembled on a plastic backing layer, sequentially with a 2 mm overlap to ensure solution migration as shown in Scheme 1A, and then assembly membrane cut into 4 mm wide strips using a paper cutter. The strips with lines were dried at 37 °C for 1 h, stored at 4 °C in a dry state until use. For quantitative measurement, the Raman intensity of the test line was collected and analyzed by the Raman instrument.

2.5. SERS measurement

100 μL of diluted sample solutions were pipetted onto the sample pad of the strips. The solution will flow by the capillary force, forcing the excessive SERS tags migrate until be captured by goat anti-mouse antibody on the C line. A red band on the C line means the SERS LFA is working properly. The color change of the T lines depended on the concentration of IL-6 antigen in samples. IL-6 antigen can interact with SERS tags to form complexes, and the complexes captured by IL-6 antibody on the T line. The target analytes on T line can be confirmed by both the color changes and the SERS signal intensity changes. The quantitative detection of target analytes is realized measuring SERS signals of SERS tags on test lines. SERS measurements were performed using a DXR Raman microscope (Thermo Scientific) with a laser wavelength at 785 nm. All spectra were obtained under the same conditions, in which the power of laser was kept at 1 mW and the exposure time was 5 s. Each SERS spectrum was averaged from 5 measurements. Results were given as means ± the standard deviation (SD). All Raman experiments were carried out at room temperature.

2.6. Instruments

SERS measurements were performed using a DXR Raman microscope (Thermo Scientific) with a laser wavelength at 785 nm. Fourier Transform Infrared spectroscopy (FT-IR) measurements were made on a FT-IR Spectrometer TENSOR 27 (Bruker Optik GmbH, Germany). Scanning electron microscopy (SEM) measurements were made on a XL30 ESEM FEG scanning electron microscope (Thermo Scientific) at an accelerating applied potential of 20 kV. All the experiments were carried out at ambient temperature.

3. Results and discussion

The synthesized Au NPs were composed of a silica particle (SiO2) core and a gold shell. Au NPs dripped onto an aluminum foil and characterized by SEM are shown in Fig. 1. Au NPs were prepared with H_2O_2 aided seed-mediated synthesis approach as described previously (Chen et al., 2011). As shown in Fig. 1B, SiO_2/Au NPs composites were successfully fabricated *via* assembling small gold particles on the surface of SiO_2 NPs. H_2O_2 was used to reduce $AuCl_4^-$ to Au^0 and enlarge the gold particles on the SiO_2/Au NPs surface, to form a gold shell and increase the outer shell thickness. As shown in Fig. 1C, large quantities of Au NPs with an average diameter of about 160 nm were obtained. Fig. 1D shows the resulting solution of colloidal particles was filtered and characterized by an absorption maximum at 700 nm using a Shimadzu UV–vis–near-infrared spectrometer. The successful fabrication of Au NPs can be directly demonstrated by Energy-dispersive X-ray (EDX) spectrum and SEM image shown in Fig. 1E. Au NPs were prepared with H_2O_2 aided seed-mediated synthesis approach (Chen et al., 2011), SiO_2/GNPs core-shell NPs were successfully fabricated *via* assembling small gold particles on the surface of SiO_2 NPs. H_2O_2 was used to reduce $AuCl_4^-$ to Au^0 and enlarge the gold particles on the SiO_2/Au NPs surface, to form a gold shell and increase the outer shell thickness. Once complete gold shell forms, the additional deposition of gold only caused the increase of the outer shell thickness, as shown in the TEM image below. Combination with EDX spectrum, we can find that a dense gold shell is wrapped around the silicon core, and only gold elements can be detected by SEM and EDX spectrum. In addition, the uniformity and the reproducibility of the SERS tags were tested in Fig. 1F and G. SERS spectra of SERS tags were detected 50 times in 3 independent batches in Fig. 1F, indicating good reproducibility of SERS tags. In order to better compare the SERS intensity difference, SERS tags were also detected for 50 times in 3 independent batches at 1332^{-1} cm with a deviation of 3.1%, shown in Fig. 1G, indicating the good reproducibility. And the surface enhancement factor (EF) of the SERS tags is $1.5 \times 10^{7\cdot}$, calculated as reported (Wang et al., 2015) (see Supporting information).

The SERS-LFA with Raman reporters were used to measure various concentrations of IL-6 in the PBS buffer. Fig. 2A shows the DTNB SERS spectra and the corresponding calibration curve (Fig. 2B). The calibration curve in Fig. 2B was obtained by plotting the SERS peak intensity at 1332 cm^{-1} from DTNB as a function of the logarithmic concentration of human IL-6. The limit of detection (LOD) was determined at the signal-to-noise ratio of 3, which was 1 pg/mL for the SERS-LFA. In short, the DTNB SERS LFA exhibited higher sensitivity and lower LOD.

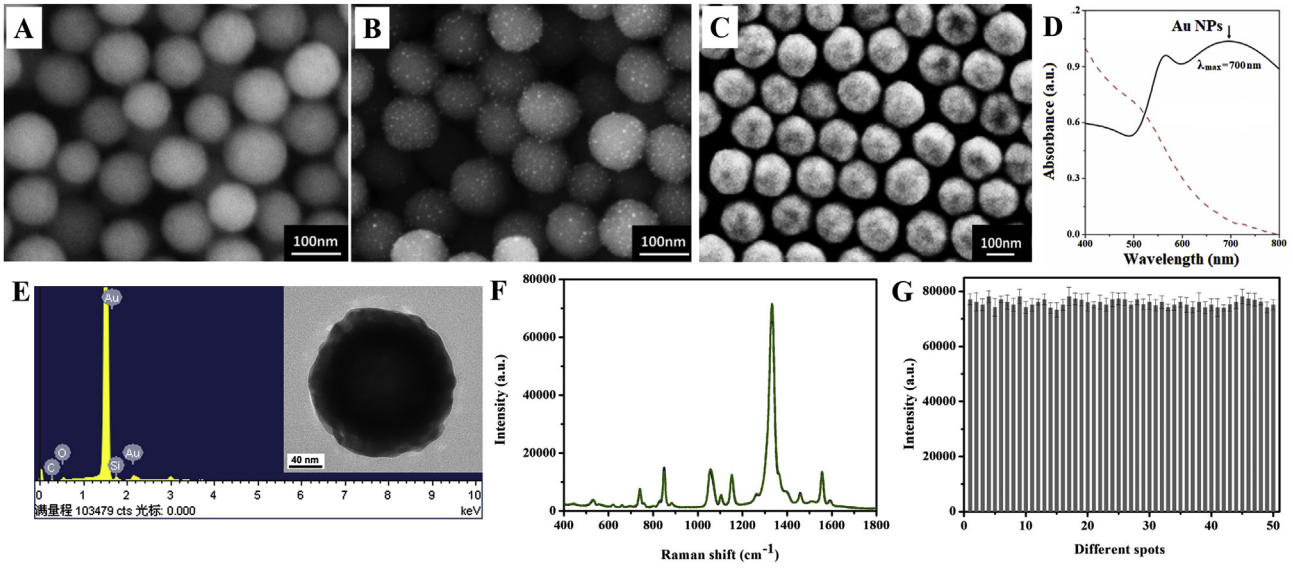

Fig. 1. SEM image of synthesis AuNPs. (A) Silica particle (SiO2) of approximate 100 nm; (B) gold nanoparticles bind to the surface of Silica particle; (C) AuNPs with core-shell structure of approximate 160 nm. (D) UV–visible spectra of AuNPs. (E) EDX spectra of AuNPs. (F) SERS spectra of SERS tags and (F) SERS intensity of tags at 1332 cm^{-1} were detected 50 times in 3 independent batches. (For interpretation of the references to color in this figure legend, the reader is referred to the Web version of this article.)

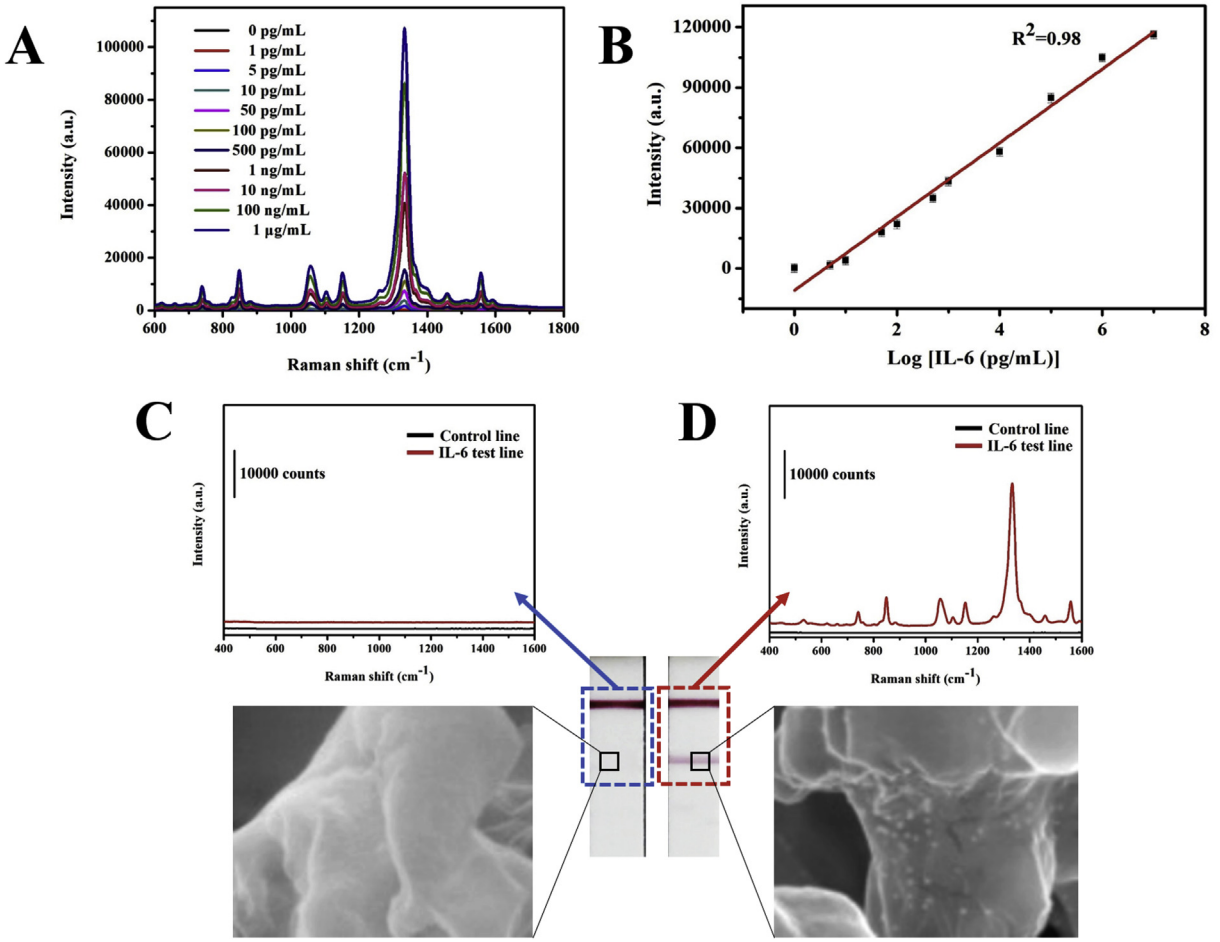

Fig. 2. (A) SERS spectra on test lines for increasing concentrations of IL-6 antigen (from 1 pg/mL to 1 μg/mL) (B) Corresponding calibration curve of SERS peak intensity at 1332 cm^{-1} versus the logarithm value of IL-6 concentration. Typical photographic image, SERS spectra and SEM images of the SERS-based lateral flow strip in the absence (C) and presence (D) of IL-6 (50 ng/mL).

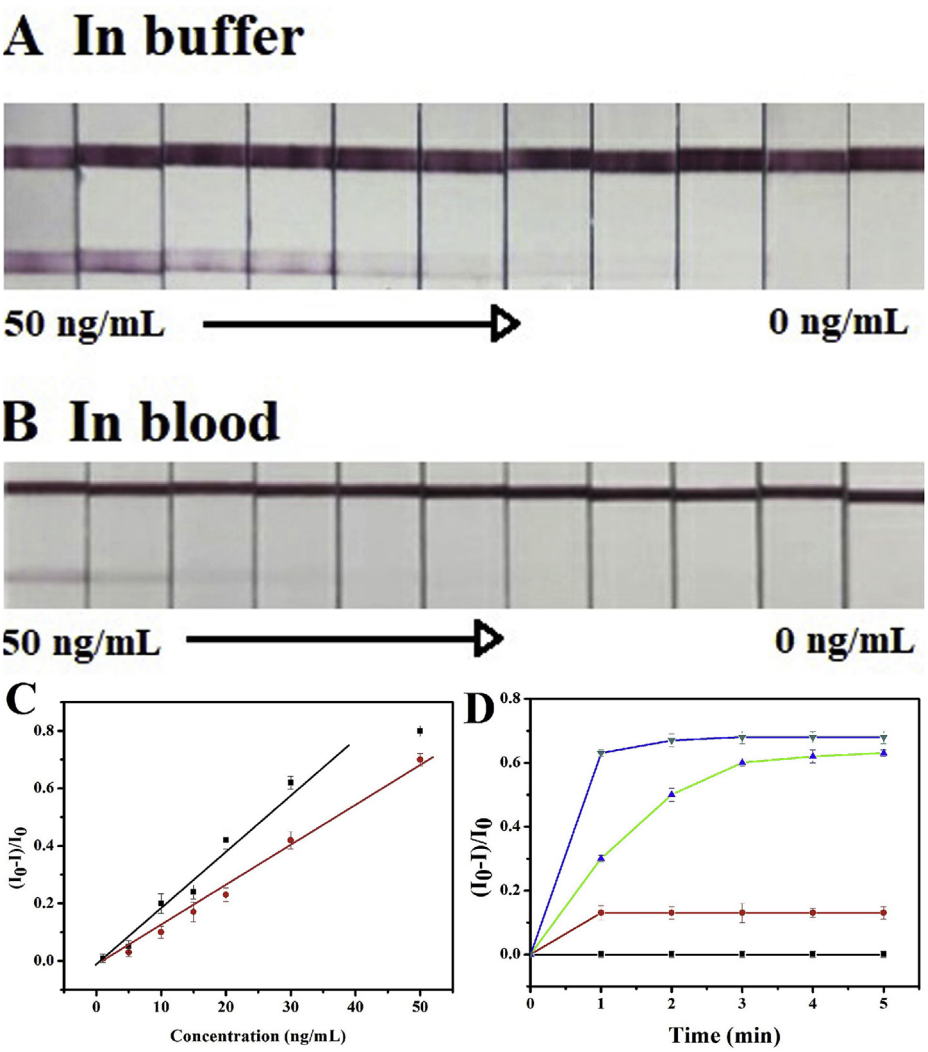

Fig. 3. Optical photos and calibration curves of colorimetric SERS-FLA for detection of IL-6 (0–50 ng/mL): (A) in PBS buffer and (B) in a mixture of 90% PBS and 10% blood plasma; (C) The difference values of SERS signal at 1332 cm^{-1} as varying concentration of IL-6 in PBS (black squares) and unprocessed whole blood (red circles) solutions. (D) The measured SERS signal at 1332 cm^{-1} responses to the reaction time with the IL-6 in PBS (blank), without (blue) and with the IL-6 (green) in the 90% PBS and 10% blood plasma, and the unprocessed whole blood solution (red) with the IL-6 concentration of 50 ng/mL. (For interpretation of the references to color in this figure legend, the reader is referred to the Web version of this article.)

In order to verify that the SERS signals were from the SERS tags combined on the T line, SERS-based LFA characterized by SEM image. In the image of Fig. 2C shows no color change, no SERS signal change and no Au NPs observed in the T line of LFA when without IL-6 present in a sample. Samples contain IL-6 recognized by SERS tags, then captured on the T line, and can be identified visually through a color change. The presence of Au NPs can be observed under the SEM image, and the intensity change of the SERS signal can also be detected (shown in Fig. 2D).

Comparative studies were performed on the colorimetric and SERS-LFA. Fig. 3A shows that the colorimetric SERS LFA worked well when it was used to measure IL-6 in the PBS solution range from 0 to 50 (0, 1, 2, 5, 10, 15, 20, 25, 30, 40, 50) ng/mL. However, when the colorimetric SERS LFA was employed for IL-6 detection in a mixture of 90% PBS and 10% unprocessed whole blood, the color intensity of the test line was much weaker than that tested in a PBS buffer (Fig. 3B). When the SERS-LFA was used for detection of IL-6 in 100% PBS solution, which was 1 order of magnitude lower than that of colorimetric LFA. In contrast, when they were applied to the sample matrix containing unprocessed whole blood, the SERS-LFA show much better performance than the colorimetric LFA. The SERS-LFA exhibited a LOD of 1 pg/mL, which was 3 orders of magnitude lower than that (50 ng/mL) of the colorimetric counterpart. This result demonstrated that the SERS-LFA had much better anti-interference ability than the colorimetric counterpart when they were applied to the blood plasma sample matrix. Fig. 3C shows the IL-6 concentration dependent SERS signal ($(I_0–I)/I_0$) in PBS or unprocessed whole blood samples. The I_0 and I refer to the SERS signal with the Raman shift at 1332 cm^{-1} without and with the IL-6 in the analyte solutions, respectively. The change of SERS signal refers to the difference between the SERS signal in the absence and presence of IL-6. SERS FLA were also used to dynamically observe the reaction process to try to reveal the origin of the discrepancy in different solutions: PBS and the unprocessed whole blood. The dynamic curves are shown in Fig. 3D. The results demonstrate the association ability is the strongest in PBS solution. However, after 1 min, the association ability in unprocessed whole blood is stronger than that in PBS. Comparing the unprocessed whole blood with PBS, we think the complexity of blood composition blocks the interaction between anti-IL-6 antibodies and IL-6 antigens. Moreover, after 1 min the discrepancy remains almost no changes.

Under the optimal experiment condition, the developed SERS-LFA can be employed to detect various concentrations of IL-6 biomarker spiked into the unprocessed whole blood solution. It is noted that measurement of IL-6 in the unprocessed whole blood can be completed within 5 min. Baseline concentrations of IL-6 in unprocessed whole blood were measured by commercial IL-6 ELISA kit prior to IL-6 measurement. None of the tests showed any signal response, which indicated that the IL-6 content in unprocessed whole blood was lower than the LOD (20 pg/mL) of the ELISA Kit. Fig. 4 shows that the intensity of SERS peak at 1332 cm^{-1} gradually rises with increasing IL-6 concentration in unprocessed whole blood. The SERS peak intensity (y) versus the IL-6 concentration (x) with the relative coefficient (R^2) of

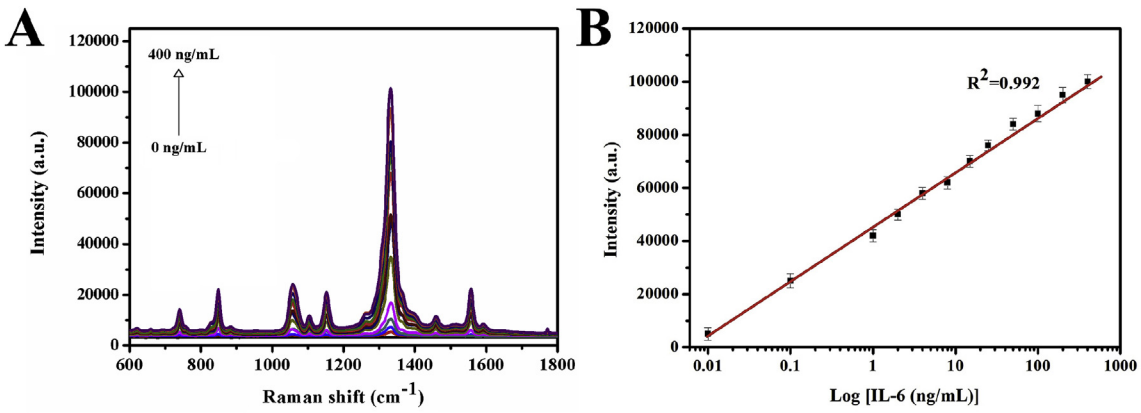

Fig. 4. (A) SERS spectra of SERS-LFA with DTNB as Raman reporter for detection of IL-6 in unprocessed whole blood, range from 0.01 to 400 ng/mL. (B) The calibration curve of SERS-LFA with DTNB as Raman reporter for detection of IL-6 in unprocessed whole blood.

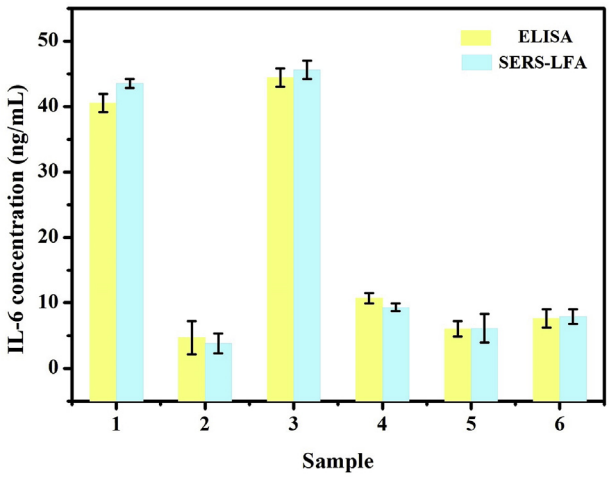

Fig. 5. IL-6 concentrations in clinical unprocessed whole blood samples, which were measured by ELISA (yellow) and the SERS-LFA (blue), respectively. (For interpretation of the references to color in this figure legend, the reader is referred to the Web version of this article.)

0.99, showing a linear detection range from 0.01 to 400 (0.01, 0.1, 1, 2, 4, 8, 15, 25, 50, 100, 200, 400) ng/mL, achieving a LOD of 5 pg/mL. The LOD was estimated with three times the standard deviation of negative control divided by the slope of calibration curve. This LOD was below the cutoff value of IL-6 concentration in unprocessed whole blood of stroke patients. Our experimental results show the SERS-LFA developed in the present work can work for IL-6 detection in unprocessed whole blood.

SERS-based LFA can achieve good analytical reproducibility of SERS signals (shown in Fig. S3). The calibrated SERS-LFA was employed to measure the IL-6 biomarker level in clinical unprocessed whole blood taken from the stroke patients. The same clinical samples were also measured with the commercial ELISA kits to validate the measurement results obtained from the SERS-LFA. Fig. 5 shows the IL-6 concentrations in six clinical unprocessed whole blood samples measured by both the SERS-LFA and the IL-6 ELISA kits methods. The results reveal that the data obtained by the SERS-LFA were comparable to those by the ELISA.

4. Conclusions

A use-friendly LFA for detection of IL-6 protein was developed based on SERS tags, shows good sensitivity, selectivity, and stability. SERS-based immunoassays are a potential alternative to ELISA. This SERS LFA extremely suitable for rapid detection to get accurate results with high selectivity in a wide concentration range. The demonstrated pg·mL^{-1} level detection will allow for the determination of IL-6 or another biomarkers in unprocessed whole blood. These merits endow the SERS-LFA platform with broad application potential in clinical diagnosis. When combined with a portable Raman spectrometer, SERS-based LFA can be employed as a POCT tool for monitoring the protein biomarkers in real samples, perform bedside detection in immune disorders, cardiovascular disease, stroke, diabetes, etc. More portability and accurate are needed for this platform form lab to clinic, is still a long way to go.

Conflict of interest statement

All authors declare that there is no conflict of interest, all authors made contribution to this work.

CRediT authorship contribution statement

Ying Wang: Writing - review & editing. **Jingyi Sun:** Writing - review & editing, Formal analysis. **Yajun Hou:** Writing - review & editing, Formal analysis, Writing - review & editing. **Cheng Zhang:** Writing - review & editing, Formal analysis, Writing - review & editing. **Dawei Li:** Writing - review & editing, Formal analysis, Writing - review & editing. **Hanxia Li:** Writing - review & editing, Formal analysis, Writing - review & editing. **Mingfeng Yang:** Writing - review & editing. **Cundong Fan:** Writing - review & editing. **Baoliang Sun:** Writing - review & editing.

Acknowledgements

This work was supported in part by funds from the National Natural Science Foundation of China (Grant No., 81471212, 81701179,81501106and 81271275), Taishan Scholars Project of Shandong Province, Development Plan of Science and Technology of Traditional Chinese Medicine in Shandong (Grant No.2017-245); the Natural Science Foundation of Shandong (Grant No. ZR2012HZ006).

Appendix A. Supplementary data

Supplementary data to this article can be found online at https://doi.org/10.1016/j.bios.2019.111432.

References

Chen, Q., Rao, Y., Ma, X., Dong, J., Qian, W., 2011. Anal. Methods 3, 274–279.
Chen, S., Dong, L., Yan, M., Dai, Z., Sun, C., Li, X., 2018. R. Soc. Open Sci. 5, 171488.
Corsini, E., House, R.V., 2018. Evaluating cytokines in immunotoxicity testing. In: Dietert, R. (Ed.), Immunotoxicity Testing. Humana Press, New York, NY, pp. 297–314.
Fu, X., Cheng, Z., Yu, J., Choo, P., Chen, L., Choo, J., 2016. Biosens. Bioelectron. 78,

530–537.
Gregersen, P.K., Behrens, T.W., 2006. Nat. Rev. Genet. 7, 917–928.
Guerrini, L., Arenal, R., Mannini, B., Chiti, F., Pini, R., Matteini, P., Alvarez-puebla, R.A., 2015. ACS Appl. Mater. Interfaces 7, 9420–9428.
Hwang, J., Lee, S., Choo, J., 2016. Nanoscale 8, 11418–11425.
Kamińska, A., Winkler, K., Kowalska, A., Witkowska, E., Szymborski, T., Janeczek, A., Waluk, J., 2017. Sci. Rep. 7, 10656.
Khlebtsov, B.N., Bratashov, D.N., Byzova, N.A., Dzantiev, B.B., Khlebtsov, N.G., 2019. Nano Research 12, 413–420.
Li, D., Yang, M., Li, H., Mao, L., Wang, Y., Sun, B., 2019. New J. Chem. 43, 5925–5931.
Lopez, A., Lovato, F., Oh, S.H., Lai, Y.H., Filbrun, S., Driskell, E.A., Driskell, J.D., 2016. Talanta 146, 388–393.
Mao, X., Xu, H., Zeng, Q., Zeng, L., Liu, G., 2009. Chem. Commun. 21, 3065–3067.
Pang, Y., Wang, C., Lu, L.C., Lu, L., Wang, C., Sun, Z., Xiao, R., 2019. Biosens. Bioelectron. 130, 204–213.
Parkin, J., Cohen, B., 2001. The Lancet 357, 1777–1789.
Rong, Z., Xiao, R., Xing, S., Xiong, G., Yu, Z., Wang, L., Jia, X., Wang, K., Cong, Y., Wang, S., 2018. Analyst 143, 2115–2121.
Russell, C., Ward, A.C., Vezza, V., Hoskisson, P., Alcorn, D., Steenson, D.P., Corrigan, D.K., 2019. Biosens. Bioelectron. 126, 806–814.
Shi, J.J., He, T.T., Jiang, F., Abdel-Halim, E.S., Zhu, J.J., 2014. Biosens. Bioelectron. 55, 51–56.
Tharion, J., Satija, J., Mukherji, S., 2015. Plasmonics 10, 753–763.
Tran, V., Walkenfort, B., König, M., Salehi, M., Schlücker, S., 2019. Angew. Chem. Int. Ed. 58, 442–446.
Van Hooij, A., Fat, E.M.T.K., Richardus, R., Van Den Eeden, S.J., Wilson, L., De Dood, C.J., Faber, R., Alam, K., Richardus, J.H., Corstjens, P.L.A.M., Geluk, A., 2016. Sci. Rep. 6, 34260.
Wang, Y.L., Salehi, M., Schutz, M., Rudi, K., Schlucker, S., 2013. Analyst 138, 1764–1771.
Wang, Y., Sun, J., Yang, Q., Lu, W., Li, Y., Dong, J., Qian, W., 2015. Analyst 140, 7578–7585.
Wang, X., Choi, N., Cheng, Z., Ko, J., Chen, L., Choo, J., 2017. Anal. Chem. 89, 1163–1169.
Wang, R., Kim, K., Choi, N., Wang, X., Lee, J., Jeon, J., 2018a. Sensor. Actuator. B Chem. 270, 72–79.
Wang, Y., Zhao, P., Mao, L., Hou, Y., Li, D., 2018b. RSC Adv. 8, 3143–3150.
Xie, W., Zhang, D., Huang, L., Liu, B., Su, E., Chen, H.Y., Gu, Z., Zhao, X., 2018. Sensor. Actuator. B Chem. 277, 502–509.
Zhang, K., Liu, G., Goldys, E.M., 2018. Biosens. Bioelectron. 102, 80–86.
Zhao, P., Li, H., Li, D., Hou, Y., Mao, L., Yang, M., Wang, Y., 2019. Talanta 198, 527–533.